IBRO Neuroscience Reports 16 (2024) 418–427

Contents lists available at ScienceDirect

IBRO Neuroscience Reports

journal homepage: www.sciencedirect.com/journal/IBRO-Neuroscience-Reports

Research Paper

Melatonin at repeated doses alleviates hyperglycemia-exacerbated cerebral ischemia-reperfusion injury at 72 h via anti-inflammation and anti-apoptosis

Qian Xu [a], Raymond Tak Fai Cheung [a,b,*]

[a] Department of Medicine, School of Clinical Medicine, Li Ka Shing Faculty of Medicine, The University of Hong Kong, Hong Kong
[b] Research Centre of Heart, Brain, Hormone & Healthy Aging, Li Ka Shing Faculty of Medicine, The University of Hong Kong, Hong Kong

ARTICLE INFO

Keywords:
Ischemia-reperfusion
Melatonin
Neuroprotective
Normoglycemia
Rats
Type 1 diabetes mellitus

ABSTRACT

Objective: We aimed to investigate how hyperglycemia would exacerbate cerebral ischemia-reperfusion injury (CIRI) in a rat model of type 1 diabetes mellitus (T1DM) and explore the beneficial effects of multiple doses of melatonin in T1DM induced CIRI.
Method: The T1DM rat model was induced with streptozocin, and melatonin (10 mg/kg) was injected at 0.5 h before ischemia as well as at 24 and 48 h after reperfusion.
Results: When compared to normoglycemic (NG) rats, T1DM rats had hyperglycemia with weight loss before CIRI. Despite comparable degrees of ischemia and initial reperfusion, T1DM rats tended to have greater weight loss and had worse neurological deficits and larger infarct volume than NG rats up to 72 h after CIRI. Persistent activation of nuclear factor kappa-light-chain-enhancer of activated B cells (NF-κB) pathway but not of apoptosis or calpains was a crucial factor in T1DM-mediated exacerbation of CIRI at 72 h. Despite lacking effects on baseline hyperglycemia, ischemia and initial reperfusion, melatonin at multiple doses lessened post-CIRI weight loss, neurological deficits and infarct volume in T1DM rats at 72 h when compared to vehicle-treated T1DM rats with CIRI. Beneficial effects of melatonin treatment included decreased activation of NF-κB pathway, apoptosis and calpains, leading to reduced expression of inducible nitric oxide synthase and enhanced neuronal density.
Conclusion: Melatonin at multiple doses can alleviate T1DM-mediated exacerbation of CIRI at 72 h through anti-inflammation and anti-apoptosis.

1. Introduction

Stroke is a leading cause of mortality and disability worldwide (Mendelson and Prabhakaran, 2021). The annual number of strokes and stroke deaths has increased substantially during the past 3 decades (Feigin et al., 2021). Severe focal cerebral hypoperfusion due to embolism, atherosclerotic disease and other conditions such as dissection, reversible cerebral vasoconstriction syndrome, vasculitis and hypercoagulability can lead to ischemic stroke with cerebral infarction (Mendelson and Prabhakaran, 2021). As a major modifiable risk factors of ischemic stroke (Diener and Hankey, 2020), diabetes mellitus (DM) has become a modern epidemic of the world with increasing incidence and prevalence in the past decade (Forbes and Cooper, 2013). Hyperglycemia in type 2 DM is attributed to insulin resistance. Insulin deficiency from autoimmune attacks on the pancreatic islet β cells caused by a combination of genetic and environmental factors leads to hyperglycemia in type 1 DM (T1DM) (Forbes and Cooper, 2013). DM increases the risk of ischemic stroke (Forbes and Cooper, 2013; Chukwuma and Tuomilehto, 1993; Sundquist and Li, 2006), and stroke patients with TIDM have a worse prognosis and a higher risk of all-cause mortality (Hägg-Holmberg et al., 2017; Atkinson et al., 2014).

Fewer studies have used DM animals to investigate how DM and hyperglycemia would exacerbate cerebral ischemia/reperfusion injury (CIRI). Hyperglycemia catalyzes the production of advanced glycation end products (AGEs) to mediate DM-related vascular diseases (Goldin et al., 2006). Stimulation of receptors for AGEs (RAGE) activates nuclear factor kappa-light-chain-enhancer of activated B cells (NF-κB) and upregulates its target genes, leading to elaboration of downstream inflammatory mediators such as TNF-α and IL-6 (Goldin et al., 2006). The inhibitor protein alpha of NF-κB (IκBα) keeps NF-κB in an inactive state

* Corresponding author at: Department of Medicine, School of Clinical Medicine, Li Ka Shing Faculty of Medicine, The University of Hong Kong, Hong Kong.
E-mail addresses: rtcheung@hkucc.hku.hk, rtcheung@hku.hk (R.T.F. Cheung).

https://doi.org/10.1016/j.ibneur.2024.03.003
Received 2 November 2023; Received in revised form 28 January 2024; Accepted 3 March 2024
Available online 5 March 2024

sequestered in the cytoplasm by masking its nuclear localization signal. NF-κB is activated after 15 min of ischemia plus 1 h of reperfusion in T1DM rats (El-Sahar et al., 2015). Hyperglycemia in T1DM impairs mitochondrial dynamics and turnover (Audzeyenka et al., 2021). Elevated AGEs and RAGEs enhance superoxide production levels in cultured vascular endothelial cells under hyperglycemic condition (Wautier et al., 2001). Mitochondrial ROS generation releases cytochrome C and other apoptotic proteins into the cytosol to initiate the intrinsic apoptotic pathway (Broughton et al., 2009). Caspase-3 is a common downstream apoptosis effector (Smith and Schnellmann, 2012). Activation of calpains is also capable of triggering the intrinsic apoptotic pathway (Harwood et al., 2005) and increasing the mitochondrial permeability (Ding et al., 2002). Calpains activation is a marker of both necrosis and apoptosis whilst caspase-3 activation is specific for apoptosis (Wang, 2000). When compared to normoglycemic (NG) rats, we have recently reported that T1DM rats had worsened CIRI following 75 min of ischemia plus 24 h of reperfusion because of augmented NF-κB pathway activation and mitochondrial cytochrome C release (Xu and Cheung, 2023).

Melatonin, a neurohormone (Yawoot et al., 2021), has neuroprotective effects when given either as a single or multiple doses as well as before or after ischemia (Feng et al., 2017; Liu et al., 2019; Pei et al., 2003). Mitochondria is a target for neuroprotective interventions in CIRI (Christophe and Nicolas, 2006). Melatonin protects against CIRI in NG rats through anti-oxidation, anti-inflammation, and anti-apoptosis (Reiter et al., 2016; Tamtaji et al., 2019; Hardeland, 2018). Moreover, melatonin can modulate NF-κB expression (Rehman et al., 2019; Ali et al., 2020) and act as a calpain inhibitor in the central nervous system (Tamtaji et al., 2019; Samantaray et al., 2008). We have recently reported that a single intraperitoneal (IP) injection of melatonin at 10 mg/kg given at 30 min before ischemia mitigated T1DM-aggravated CIRI at 24 h via anti-inflammatory and anti-apoptotic effects (Xu and Cheung, 2023).

The present study was conducted to investigate how hyperglycemia would exacerbate CIRI in streptozocin-induced TIDM rats at 72 h of reperfusion following focal ischemia for 75 min and explore the beneficial effects of three IP doses of melatonin at 10 mg/kg given at 0.5 h before ischemia as well as at 24 and 48 h after reperfusion.

2. Methods

2.1. Animal and T1DM model

The experimental protocol was approved by the Committee on the Use of Live Animals in Teaching and Research (#4470–17), The University of Hong Kong (HKU), Hong Kong. The 3 R (replacement, reduction, refinement) principles in animal research were adhered, and the number of rats in the control or sham group which had more homogeneous results was kept to a minimum. Male Sprague Dawley rats weighing 190–210 g were purchased from the Centre for Comparative Medicine Research (CCMR), HKU, Hong Kong. CCMR regulations for the care and use of laboratory animals were applied to all experimental procedures. Rats had free access to food and water. Rats were housed and maintained on a 12-h light-dark rhythm under controlled temperature (22–24°C) for at least three days before the commencement of experimental procedures. T1DM was induced by a single IP injection of streptozotocin (STZ; 65 mg/kg, Sigma-Aldrich, St. Louis, MO, USA) freshly prepared in citrate buffer (50 mM sodium citrate, pH 4.5). Only the citrate buffer was injected into the rats of the NG control. The random glucose concentration was measured in the blood specimen obtained via the tail vein one week later using a glucometer (Accu-Chek, Roche Group, Basel, Switzerland). Rats with random blood glucose levels higher than 16.7 mmol/L were considered to have developed T1DM (Yan et al., 2012, 2018). Rats with blood glucose lower than this level after STZ injection were excluded from further procedures.

2.2. Animal grouping

NG rats undergoing sham middle cerebral artery occlusion (MCAO) were used as a control and categorized as NG sham group. NG CIRI group was comprised of NG rats undergoing MCAO. T1DM rats undergoing sham MCAO were categorized as T1DM sham group, and T1DM CIRI group was comprised of T1DM undergoing MCAO. Furthermore, T1DM CIRI rats treated with multiple injections of either vehicle or melatonin were categorized as T1DM CIRI vehicle-treated group and T1DM CIRI melatonin-treated group, respectively. The number of animals per group in each experiment was indicated in the text or figure legends.

2.3. Drug administration

Some T1DM rats undergoing MCAO were randomly assigned to receive either melatonin or the vehicle. Multiple IP injections of melatonin (10 mg/kg) or the vehicle were given at 30 min before as well as at 24 and 48 h after MCAO onset. Melatonin (Sigma-Aldrich) was first dissolved in dimethyl sulfoxide (DMSO; Sigma-Aldrich) before dilution using normal saline with a final concentration of DMSO less than 5%. The random glucose concentration was measured in the blood specimen obtained from the tail vein shortly before sacrifice.

2.4. Right-sided endovascular MCAO

CIRI was achieved by right-sided endovascular MCAO for 75 min followed by reperfusion for 72 h. Two weeks after IP injection of streptozotocin or citrate buffer, T1DM or NG rats underwent real or sham endovascular MCAO. Body weights were measured before real or sham MCAO as well as at 24, 48 and 72 h after real or sham reperfusion. Briefly, rats were anaesthetized with an IP injection of a mixture of ketamine (67 mg/kg; Alfasan International B.V., Woerden, Netherlands) plus xylazine (6.7 mg/kg; Alfasan International B.V.). The right carotid arteries were exposed, and the right external carotid artery (ECA) was isolated distally after dividing its branches using bipolar electric coagulation (GN60, Aesculap AG & Co, Hesse, Germany). Micro-clips were temporarily applied to both the right common carotid artery and right internal carotid artery (ICA). To occlude the right middle cerebral artery (MCA) at its origin, a piece of 4-o monofilament nylon suture (4037PK5Re, Doccol Corporation, Sharon, MA, USA) was inserted into the right ICA lumen around 18–20 mm from the carotid bifurcation. The nylon suture was withdrawn carefully after focal ischemia to achieve reperfusion. Rats of the NG sham group and T1DM sham group underwent sham MCAO procedures which were identical to those of MCAO with the exceptions of occlusion of the MCA and absence of reperfusion. After real or sham MCAO procedures, the neck incision was closed, and the rats were allowed to recover from the anaesthesia. Buprenorphine (50 μg/kg every 12 h; Reckitt Benckiser Healthcare Ltd, Hull, UK) was given subcutaneously for relief of postoperative pain. Enrofloxacin (10 mg/kg; Bayer Ltd, Kiel, Germany) was given intramuscularly to prevent wound infection. Rectal temperature was kept at 37.0 ± 0.5°C using a rectal thermostat probe and a thermostatically regulated heating pad. The heart rate and respiratory rate were monitored every 20–30 min during MCAO. At 72 h after real or sham reperfusion, the rats were sacrificed with an IP injection of pentobarbital (100 mg/kg; Alfasan International B.V.) for further molecular testing or infarct volume calculation. Rats with any one of the following were excluded from this study: failed induction of CIRI; excessive weight loss; distress despite analgesic usage; and death before sacrifice.

2.5. Monitoring of the regional cerebral blood flow (CBF)

While under anaesthesia for the endovascular MCAO, a burr hole was made on the skull located at 2 mm posterior and 5 mm lateral to the bregma on the right side for regional CBF monitoring using a laser

Doppler flowmeter (MBF3D, Moor Instruments Limited, Axminster, Devon, UK). Successful induction of MCAO was indicated by a drastic decline in the regional CBF to less than 35% of the baseline values. A surge in regional CBF to more than 80% of the baseline values upon withdrawal of the nylon suture would reveal adequate reperfusion. Regional CBF data at onset, 30 and 60 min of ischemia as well as upon reperfusion were expressed as percentages of the baseline values for analysis.

2.6. Modified neurological severity score (mNSS)

Neurobehavioral performance in motor and sensory functions, reflexes and balance was assessed using the mNSS (Lee et al., 2014; Schaar et al., 2010). One point would be assigned for the incomplete achievement of a test item. Higher points would indicate a more severe neurological deficit with a maximum of 18 points and zero point in healthy rats. The mNSS test was applied to the rats at 72 hours after real or sham CIRI.

2.7. Rotarod test

Three days before real or sham MCAO, some rats were daily placed onto a rotating treadmill (10 revolutions per min; HKU) (Söderpalm et al., 1989; Barone et al., 1992). Rats incapable of maintaining themselves on the rotating treadmill for at least 5 min during training were excluded. Five min were taken as the baseline latency to fall off. The test was repeated at 24, 48 and 72 h of real or sham reperfusion.

2.8. Edema-adjusted brain infarct volume

The brain between +4 and –8 mm bregma level was cut into 2-mm thick coronal slices. Slices were reacted with 1.5% triphenyl tetrazolium chloride (Sigma-Aldrich) solution to reveal the infarct. Digital photographs of the coronal slices were obtained by a scanner for infarct size measurement using the Image J system (Image J, v1.51m9, National Institutes of Health, USA). The edema adjusted (EA)-infarct volume was derived from the integrated infarct volume multiplied by the ratio between contralateral and ipsilateral hemispheric volumes (Nouraee et al., 2019).

2.9. Western blot

Cortical brain regions between +2 and –2 mm bregma levels were collected for homogenization. Protein samples were separated by 10–15% sodium dodecyl sulphate–polyacrylamide gel electrophoresis and then transferred to polyvinylidene fluoride (PVDF) membranes (Bio-Rad, Hercules, USA). The PVDF membranes were blocked with 10% non-fat milk (Bio-Rad) for 1 h at room temperature and then incubated with primary antibodies in 5% non-fat milk overnight at 4 °C. The membranes were then incubated with corresponding secondary antibodies for 2 h at room temperature for detection of phosphorylated IκBα (p-IκBα), total IκBα, cytochrome C, α-II-spectrin (α-fodrin) breakdown product (SBDP) and β-actin.

The ratio of p-IκBα to total IκBα would indicate NF-κB activation (Viatour et al., 2005). Calpain-mediated specific proteolysis of α-II-spectrin would generate 145 kilodalton (kDa) SBDP whilst caspase-3-mediated specific proteolysis of α-II-spectrin would generate 120 kDa SBDP (Wang, 2000; Zhang and Bhavnani, 2006). The blots were imaged with Enhanced Chemiluminescent reagents (GE Healthcare Life Sciences, USA) and recorded by the Imagine System (Bio-Rad). Protein expressions were analyzed using the Image J system (v1.51m9). The band intensity was adjusted according to the β-actin band and expressed as a percentage of the result of the sham or vehicle group for analysis.

Primary antibodies against p-IκBα (1:1000, 9246) and total-IκBα (1:1000, 4814) were purchased from Cell Signaling Technology (Massachusetts, USA). Primary antibodies against β-actin (1:1000, sc-81178) and cytochrome C (1:500, sc-13561) were purchased from Santa Cruz Biotechnology (Texas, USA). Primary antibody against α-fodrin (1:4000, BML-FG6090) was purchased from Enzo Life Science (New York, USA). Horseradish peroxidase-conjugated rabbit anti-mouse secondary antibody (1:2000, Nr.P0260) was purchased from Dako (Glostrup, Denmark). Horseradish peroxidase-conjugated goat anti-rabbit secondary antibody (1:2000, sc-2357) was purchased from Santa Cruz Biotechnology.

2.10. Immunofluorescence staining

Anaesthetized rats were transcardially perfused with pre-cooled phosphate-buffered saline (PBS) and then 4% paraformaldehyde (PFA; pH 7.4) for initial fixation. Brains were fixed overnight in 4% PFA at 4 °C and cryoprotected using 10, 20 and then 30% sucrose in PBS for three days. Ten μm thick coronal cryosections were obtained from three bregma levels (–1.5, 0 and +1.5 mm). Three brain sections per rat (with one brain section per bregma level) were affixed on Superfrost Plus slides (Menzel-Glaser, Braunschweig, LS, Germany) and air-dried overnight. The slides were boiled in citrate buffer (50 mM; pH 6.5) for 10 min to retrieve the antigen. After cooling, non-specific binding was blocked with 10% goat serum at room temperature for 1 h. Brain sections were then incubated with the primary antibody in 3% goat serum at 4 °C overnight and then incubated with the corresponding secondary antibody at room temperature to detect inducible nitric oxide synthase (iNOS), cluster of differentiation (CD)-68 and neuronal nuclear protein (NeuN).

iNOS and CD-68 would be markers for pro-inflammatory macrophage/microglia (Chistiakov et al., 2017). NeuN would label surviving neurons. Slides were coverslipped with mounting medium 4′,6-diamidino-2-phenylindole dihydrochloride (DAPI; Invitrogen, Waltham, Massachusetts, USA). Five photomicrographs per bregma level were randomly taken over the right hemispheric areas at 100X magnification using a fluorescence microscope (Nikon, Tokyo, Japan). The number of positively stained cells was counted using Image J software (Image J, v1.51m9). Cell density was derived from the average number of positively stained cells per high power field and expressed as a percentage of the result of the vehicle group for analysis.

Primary antibody against CD-68 (1:500) was purchased from AbD Serotec (Oxford, United Kingdom). Primary antibody against iNOS (1:100, sc-651) was purchased from Santa Cruz Biotechnology. Primary antibody against NeuN (1:500, MAB377) was purchased from Merck Millipore (Massachusetts, USA). Alexa Fluor®488 goat anti-mouse (1:500) and Alexa Fluor®594 mouse anti-rabbit (1:500) were purchased from Merck Millipore.

2.11. Terminal deoxynucleotidyl transferase dUTP nick end labelling (TUNEL) staining

The in situ cell death detection kit (Roche, Branchburg, NJ, USA) was used to detect TUNEL+ apoptotic cells. As for immunofluorescence staining, brain sections at three bregma levels per rat were affixed on Superfrost Plus slides (Menzel-Glaser) and air-dried overnight. The slides were boiled in citrate buffer (50 mM; pH 6.5) for 10 min to retrieve the antigen. After cooling, 3% H_2O_2 was added as the blocking solution for 10 min before incubating with the freshly prepared permeabilization solution (0.1% Triton X-100 in 0.1% sodium citrate) for 2 min on ice. Next, the TUNEL reaction mixture was prepared and applied to slides for 60 min. Five photomicrographs at the bregma levels were randomly taken over the right hemispheric areas at 400X magnification using a fluorescence microscope (Nikon). The number of positively stained cells was counted using Image J software (Image J, v1.51m9). Cell density was derived from the average number of positively stained cells per high power field and expressed as a percentage of the result of the vehicle group for data analysis.

2.12. Statistical analysis

All data were shown in the mean ± standard error of the mean (SEM). Student's t-test was used to compare the differences between two groups. Analysis of variance (ANOVA) with subsequent Student-Newman-Keuls or Dunnett T3 post-hoc test was used to compare the differences among three or more groups. Data on regional CBF were analyzed using general linear model two-way repeated measures ANOVA followed by Tukey's HSD or Games-Howell post-hoc test. Body weight changes and rotarod latency over different time points were analyzed using general linear model two-way repeated measures ANOVA. SPSS 27 was used for all statistical analyses. A two-tailed P value <0.05 was used to infer statistical significance.

3. Results

3.1. T1DM-exacerbated CIRI at 72 h

The experimental design is shown in Fig. 1A. STZ-injected rats had higher blood glucose levels (30.1 ± 1.0 mmol/L, n=15; P<0.001) and lower body weight (296.7 ± 6.4 g; P<0.001) when compared with citrate buffer-injected NG rats (7.9 ± 0.3 mmol/L; 349.9 ± 6.6 g; n=8), indicating the successful induction of T1DM model. MCAO for 75 min followed by 72 h of reperfusion was used to produce CIRI in NG and T1DM rats. Regional CBF decreased to less than 35% of the baseline upon suture insertion (0 min; P<0.001 vs baseline level) and returned to more than 80% of the baseline level upon suture withdrawal (reperfusion; Fig. 1B; no significant difference from baseline level), confirming the successful induction of CIRI. CIRI led to a significant weight loss at 24 h of reperfusion (P<0.05 vs initial body weight) with subsequent stabilization till 72 h in both the NG CIRI group and T1DM CIRI group (Fig. 1C), and the weight changes were not significant in both the NG sham group and T1DM sham group. CIRI generated focal brain infarct (Figs. 1F and 1G; P<0.001), decreased latency to fall off (Fig. 1D; P<0.001) and neurological deficits on mNSS (Fig. 1E; P<0.001) in both NG CIRI group and T1DM CIRI group when compared to NG sham group and T1DM sham group, respectively. Post-CIRI weight loss was significantly worse in T1DM CIRI group than NG CIRI group (Fig. 1C; P<0.05). Moreover, T1DM led to exacerbations in EA-infarct volume (Figs. 1F and 1G; P<0.001), decreased latency to fall off (Fig. 1D; P<0.001) and the mNSS score (Fig. 1E; P<0.001) in T1DM CIRI group when compared to NG CIRI group.

3.2. T1DM-exacerbated CIRI alleviated by repeated doses of melatonin

Repeated IP doses of melatonin (10 mg/kg) were given at 30 min before ischemia as well as at 24 and 48 h after reperfusion to randomly selected T1DM rats (Fig. 1A). Regional CSF changes during ischemia and upon reperfusion were similar among all three groups (Fig. 1B). Repeated doses of melatonin had no influence on post-stroke blood glucose (T1DM CIRI vehicle-treated group, n=5, 22.6 ± 10.2 mmol/L; T1DM CIRI melatonin-treated group, n=5, 28.2 ± 6.1 mmol/L) and tended to lessen post-CIRI weight loss so that the body weight of T1DM CIRI melatonin-treated group was not significantly different from that of NG CIRI group (Fig. 1C). Repeated doses of melatonin decreased the EA-infarct volume (Figs. 1F and 1G; P<0.001), reduced the decreased latency to fall off at 48 and 72 h after reperfusion (Fig. 1D; P<0.001), and ameliorated the mNSS score (Fig. 1E; P<0.001) in T1DM CIRI melatonin-treated group when compared to T1DM CIRI vehicle-treated group.

3.3. T1DM-exacerbated post-CIRI cerebral cortical NF-κB activation but not rise in levels of cytochrome C, caspase-3-specific 120 kDa SBDP and calpain-specific 145 kDa SBDP

Protein levels in the cerebral cortex reflecting activation of NF-κB, apoptosis and/or necrosis were compared between NG and T1DM rats with or without CIRI. T1DM *per se* did not affect p-IκBα/IκBα ratio (Fig. 2B) and cytochrome C level (Fig. 2C), caspase-3-specific 120 kDa SBDP level (Fig. 2D) and calpain-specific 145 kDa SBDP level (Fig. 2E) with no difference between NG sham group and T1DM sham group. Post-CIRI rise in p-IκBα/IκBα ratio was significant in T1DM CIRI group (Fig. 2B; P=0.001) but not NG CIRI group leading to a significant difference between them (P<0.01). Post-CIRI rise in cytochrome C level was significant in NG CIRI group (Fig. 2C; P<0.05) and T1DM CIRI group (P<0.005) without any significant difference between them. Post-CIRI rise in caspase-3-specific 120 kDa SBDP was significant in NG CIRI group (Fig. 2D; P<0.05) but not T1DM CIRI group, and there was no significant difference between them. Post-CIRI rise in calpain-specific 145 kDa SBDP was significant in NG CIRI group (Fig. 2E; P<0.01) and T1DM CIRI group (P<0.05), and there was no any significant difference between them.

3.4. T1DM-exacerbated post-CIRI cerebral cortical apoptosis and inflammation alleviated by repeated doses of melatonin

Repeated IP doses of melatonin (10 mg/kg) were given at 30 min before ischemia as well as at 24 and 48 h after reperfusion to randomly selected T1DM rats (Fig. 1A). When compared to T1DM CIRI vehicle-treated group of rats, repeated doses of melatonin alleviated post-CIRI increases in p-IκBα/IκBα ratio (Fig. 3A and B; P<0.005), cytochrome C level (Fig. 3A and C; P=0.001), caspase-3-specific 120 kDa SBDP level (Figs. 3A and 3D; P=0.001) and calpain-specific 145 kDa SBDP level (Fig. 3A and E; P<0.05) in the cerebral cortex of T1DM CIRI melatonin-treated rats. Moreover, the present regimen of melatonin treatment led to reduced densities of iNOS+ cells (Fig. 4A and B; P<0.005) and TUNEL+ apoptotic cells (Fig. 4E and F; P<0.05) but increased density of NeuN+ neuronal cells (Fig. 4G and H; P<0.001) in the cerebral cortex of T1DM CIRI melatonin-treated rats when compared to those of T1DM CIRI vehicle-treated group; there was no effect on the density of CD-68+ cells (Fig. 4C and D).

4. Discussion

Fewer studies on the treatments against CIRI have used T1DM animals (Yan et al., 2018; Cui et al., 2016). In addition, only infarct volume was compared between NG and T1DM animals without any further exploration on the underlying mechanisms of T1DM-mediated exacerbation of CIRI (Toung et al., 2000; Jouihan et al., 2013). Our recent study has reconfirmed that T1DM would worsen CIRI leading to a larger infarct and worse neurological deficits at 24 h and reported that T1DM-exacerbated CIRI was partly mediated by augmented NF-κB pathway activation and mitochondrial cytochrome C release in the cerebral cortex (Xu and Cheung, 2023). T1DM was induced by a single IP injection of STZ to destroy the pancreatic islet β cells (Furman, 2015). Moreover, a single IP dose of melatonin at 10 mg/kg given at 30 min before CIRI was found to alleviate T1DM-exacerbated CIRI at 24 h via melatonin's anti-inflammatory and anti-apoptotic effects (Xu and Cheung, 2023). As platelet adhesion and aggregation, leukocyte infiltration, oxidative stress, mitochondrial-mediated pathways and blood-brain-barrier disruption play their roles in CIRI and these processes change over time following reperfusion (Lin et al., 2016), it is pertinent to confirm any detrimental effect of T1DM at 72 h of CIRI and reveal any beneficial effect of repeated doses of melatonin at this later time point. It is also relevant to investigate the possible mechanisms contributing to T1DM-exacerbated CIRI and melatonin-mediated benefit at 72 h.

Unlike clinical studies, experimental studies using animal models can reveal underlying mechanisms of exacerbated damages attributable to T1DM and allow exploration of novel therapies. The use of STZ is different from autoimmune destruction of pancreatic β cells in human T1DM patients and so the current T1DM model replicates the

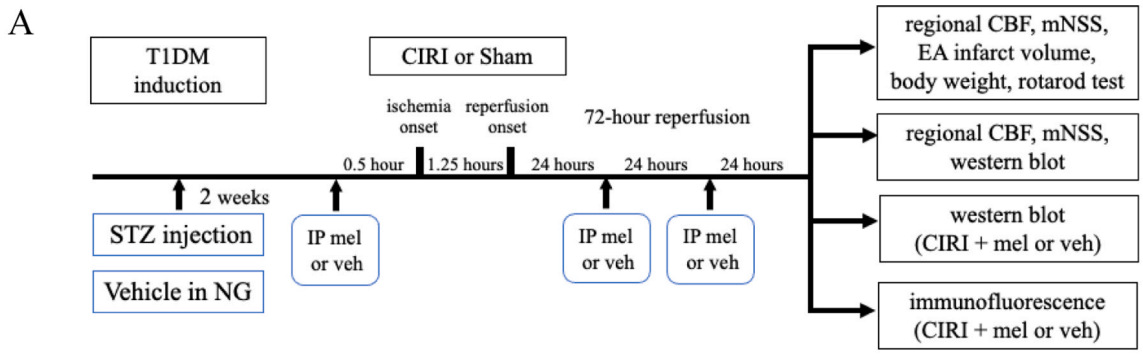

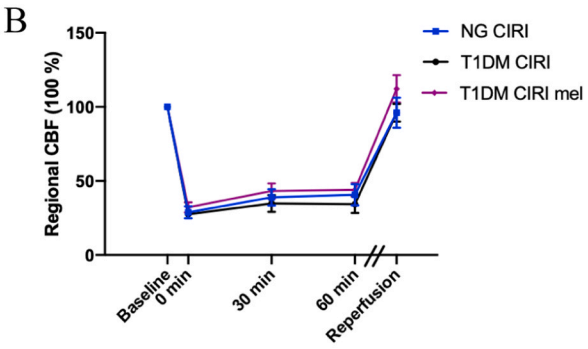

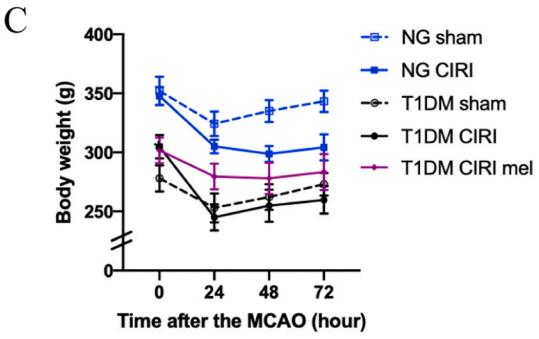

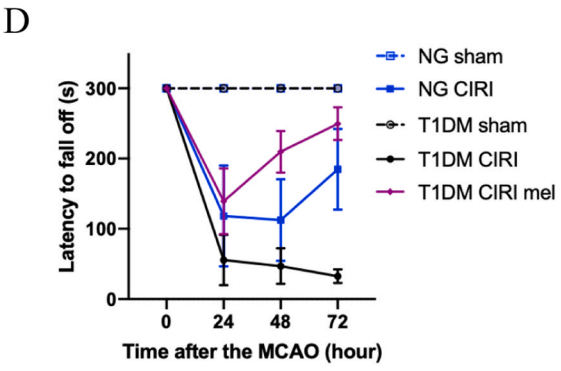

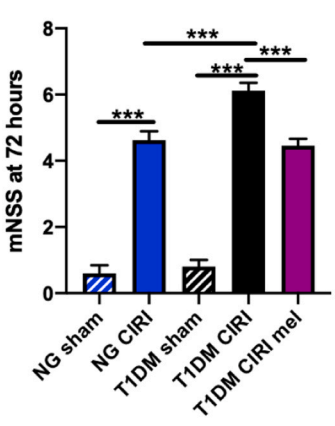

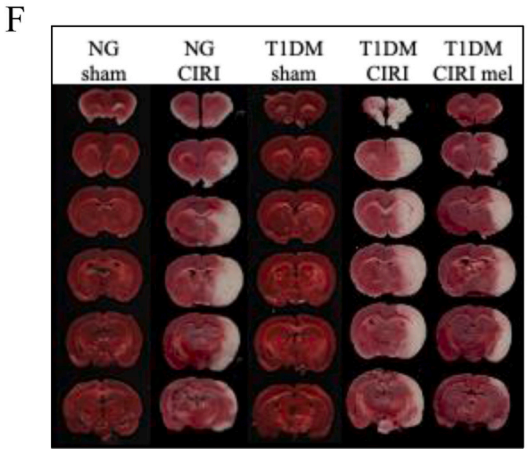

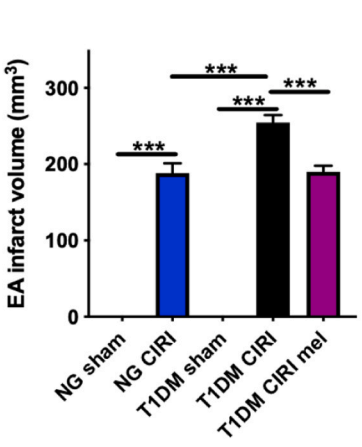

(caption on next page)

Fig. 1. Effects of T1DM with or without melatonin (mel) on regional CBF, weight loss, EA infarct volume and neurological functions at 72 h post-CIRI. (A) Experimental design with timeline. (B) Normalized regional CBF at different time points of 75-min MCAO in NG rats (NG CIRI, n=5), T1DM rats (T1DM CIRI, n=8), and T1DM rats treated with melatonin (T1DM CIRI mel, n=5). (C) Body weight at baseline, 24, 48 and 72 h of CIRI (NG sham, NG CIRI, and T1DM sham, n=4 per group; T1DM CIRI, n=6; and T1DM CIRI mel, n=5). (D) Latency to fall off in rotarod test at baseline and 24, 48 and 72 h (NG sham, NG CIRI, and T1DM sham, n=4 per group; T1DM CIRI, n=6; and T1DM CIRI mel, n=6). (E) mNSS at 72 h (NG sham, n=5; NG CIRI, n=8; T1DM sham, n=6; T1DM CIRI, n=17; and T1DM CIRI mel, n=11). (F) Representative photographs of coronal brain slices between bregma level +4 mm and –8 mm. (G) EA infarct volume at 72 h (NG sham, n=3; NG CIRI, n=4; T1DM sham, n=3; T1DM CIRI, n=5; and T1DM CIRI mel, n=5). Data were analyzed by Two-way repeated measures ANOVA followed by Tukey's HSD or Games-Howell post-hoc tests in Figures B, C and D. Data were analyzed by one-way ANOVA followed by Tukey's HSD post hoc test in Figs. E and G. * P<0.05, ** P<0.01 and *** P<0.001 between groups.

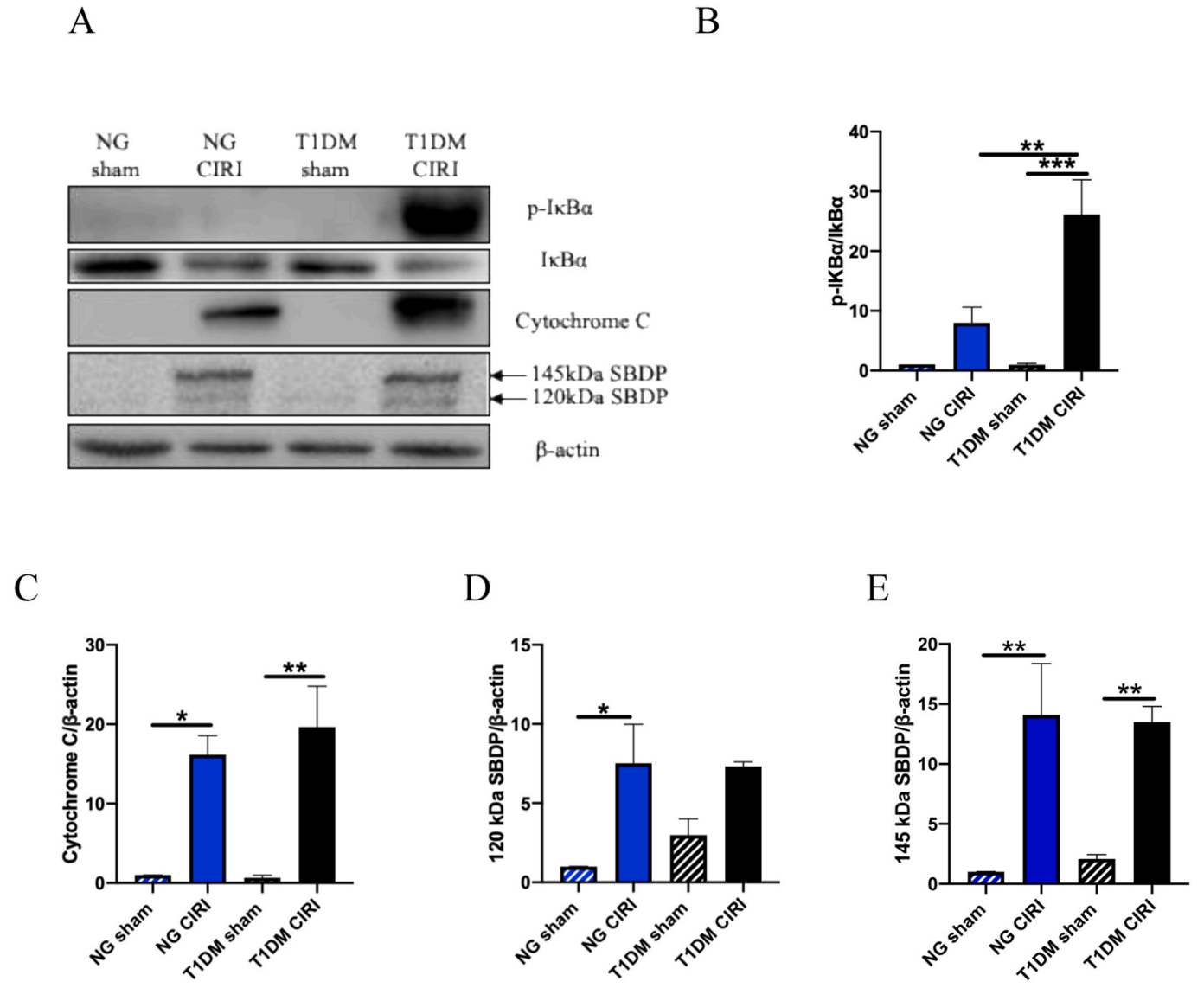

Fig. 2. Effects of T1DM on protein expression of p-IκBα, total IκBα, cytochrome C, caspase-3-specific 120 kDa, calpain-specific 145 kDa SBDP and β-actin at 72 h post-CIRI (n=4 per group). (A) Representative western blot photographs of p-IκBα, total IκBα, cytochrome C, 145 kDa SBDP, 120 kDa SBDP and β-actin. (B) p-IκBα/total IκBα ratio derived from relative intensities of western blot bands. (C) Relative intensities of cytochrome C bands. (D) Relative intensities of casepase-3-specific 120 kDa bands. (E) Relative intensities of calpain-specific 145 kDa SBDP bands. Data were analyzed by one-way ANOVA followed by Tukey's HSD post hoc test in Figures B, C, D and E. * P<0.05 and ** P<0.01 between groups.

hyperglycemic environment from insulin deficiency only (Atkinson et al., 2014). More importantly, the duration of hyperglycemia is short in animal models, e.g. two weeks before CIRI in the present study, but DM is a chronic disease (Noshahr et al., 2020). Indeed the duration of DM is an independent risk factor for ischemic stroke (Hägg et al., 2014). A chronic hyperglycemic environment of DM is required to produce macrovascular and microvascular complications (Atkinson et al., 2014) and also promote associated metabolic conditions, such as dyslipidemia, hypertension, vascular inflammation and a prothrombotic state (Beckman et al., 2002).

In the present study, rats of T1DM CIRI group had a much larger EA-infarct volume and worse neurological deficits than those of NG CIRI group at 72 h of CIRI. In addition, post-CIRI weight loss and reduced latency to fall off in rotarod test were worse in rats of T1DM CIRI group than those of NG CIRI group. Whilst exogenous insulin replacement is the mainstay treatment in T1DM patients (Atkinson et al., 2014), studies

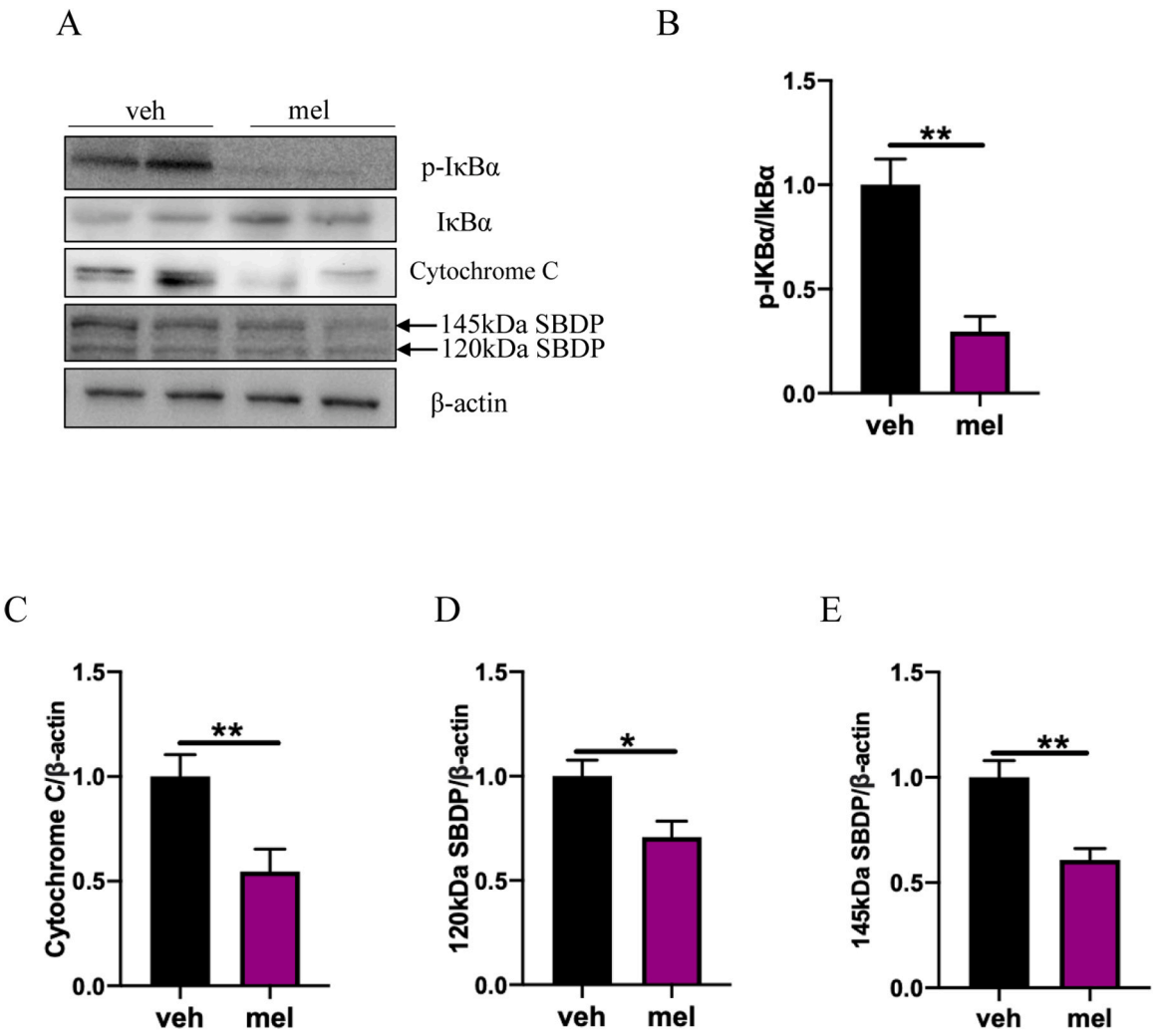

Fig. 3. Effects of repeated 10 mg/kg doses of melatonin (mel) or its vehicle (veh) (given at 30 min before and repeated at 24 and 48 h after CIRI) on cerebral cortical protein expression of p-IκBα, total IκBα, cytochrome C, caspase-3-specific 120 kDa, calpain-specific 145 kDa SBDP and β-actin at 72 h post-CIRI in T1DM rats. (A) Representative western blot photographs of p-IκBα, total IκBα, cytochrome C, 145 kDa SBDP, 120 kDa SBDP and β-actin. (B) p-IκBα/total IκBα ratio derived from relative intensities of western blot bands (n=4 per group). (C) Relative intensities of cytochrome C bands (T1DM CIRI vehicle-treated group, n=7; and T1DM CIRI melatonin-treated group, n=8 per group). (D) Relative intensities of western blot bands for 120 kDa SBDP (T1DM CIRI vehicle-treated group, n=7; and T1DM CIRI melatonin-treated group, n=8), (D) Relative intensities of calpain-specific 145 kDa SBDP bands (T1DM CIRI vehicle-treated group, n=7; and T1DM CIRI melatonin-treated group, n=8). * $P<0.05$ and ** $P<0.005$ between groups.

have shown that intensive treatment of hyperglycemia in DM patients can reduce the risk of microvascular complications but not for stroke (Diener and Hankey, 2020). Current acute stroke guidelines acknowledge limited data from clinical trials and recommend close monitoring of blood glucose with avoidance of both hyperglycemia and hypoglycemia.

When compared with the respective sham groups, published (Xu and Cheung, 2023) and current data showed that CIRI would lead to persistent cerebral cortical activation of NF-κB in rats of T1DM CIRI groups but not NG CIRI groups at 24 and 72 h post-CIRI. In addition, the ratio of p-IκBα/IκBα in the cerebral cortex increased significantly in rats of T1DM CIRI groups when compared to NG CIRI groups at these time points (published (Xu and Cheung, 2023) and current data). As persistent NF-κB activation may play a critical role in T1DM-mediated exacerbation of CIRI at 72 h, attempts to suppress NF-κB activation and, in turn, reduce downstream cytokines expression may be effective with a relatively long treatment time window in T1DM patients with ischemic stroke. Yet suppression of NF-κB activation should be maintained for a relatively long period post-reperfusion. iNOS expression is also under the NF-κB regulation in a time- and concentration- dependent manner. Under hyperglycemic conditions, activated NF-κB is rapidly translocated to the nucleus, resulting in increased binding to the iNOS promoter and a consequential rise in iNOS expression (Jia et al., 2013). The macrophage/microglia infiltration and the expression of iNOS as respectively detected using anti-CD-68 and anti-iNOS antibodies were reduced with a single injection of melatonin (Xu and Cheung, 2023). The reduced expression of iNOS and macrophage/microglia activation may be regulated through the decreased activation of NF-κB.

Our recent study showed elevated cerebral cortical levels of cytochrome C in both NG CIRI group and T1DM group at 24 h post-CIRI (Xu and Cheung, 2023), and these elevations were also seen in the present study at 72 h post-CIRI. Current results of elevated cerebral cortical level of caspase-3-specific 120 kDa SBDP were significant in NG CIRI group but not T1DM group at 72 h post-CIRI, but these elevations were not significant in both NG CIRI group and T1DM CIRI group at 24 h post-CIRI as recently reported (Xu and Cheung, 2023). Current results of elevated cerebral cortical levels of calpain-specific 145 kDa SBDP were significant in both NG CIRI group and T1DM CIRI group at 72 h post-CIRI, but these elevations were not significant in both NG CIRI group and T1DM CIRI group at 24 h post-CIRI as recently reported (Xu

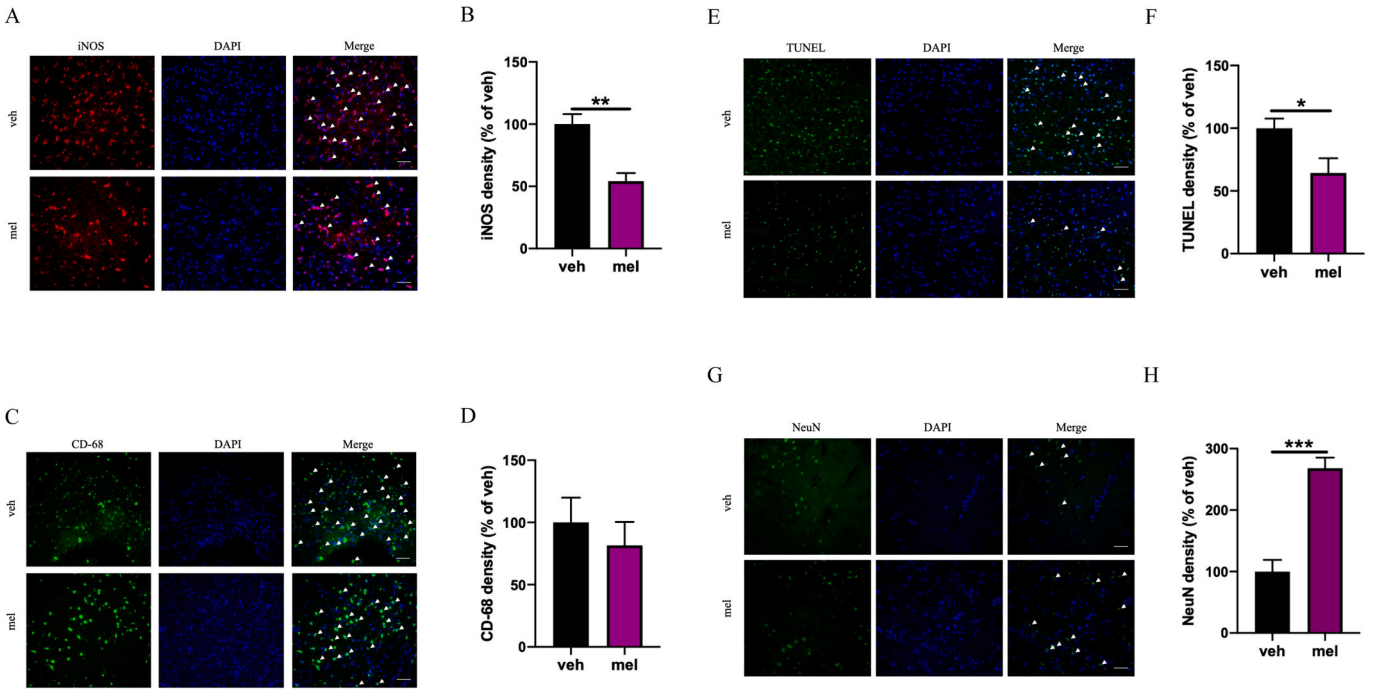

Fig. 4. Effects of repeated 10 mg/kg doses of melatonin (mel) or its vehicle (veh) (given at 30 min before and repeated at 24 and 48 h after CIRI) on immunofluorescence staining of iNOS, CD-68, TUNEL and NeuN at 72 h post-CIRI over cerebral cortex in T1DM rats. (A) Representative fluorescence photomicrographs of iNOS+ cells (scale bar=50 μm). (B) Relative iNOS+ cell density in T1DM CIRI vehicle-treated group (n=5) and T1DM CIRI melatonin-treated group (n=4). (C) Representative fluorescence photomicrographs of CD-68+ cells (scale bar=50 μm). (D) Relative CD-68+ cell density in T1DM CIRI vehicle-treated group (n=5) and T1DM CIRI melatonin-treated group (n=4). (E) Representative fluorescence photomicrographs of TUNEL+ apoptotic cells (scale bar=50 μm). (F) Relative TUNEL+ cell density in T1DM CIRI vehicle-treated group (n=5) and T1DM CIRI melatonin-treated group (n=4). (G) Representative fluorescence photomicrographs of neuN+ surviving neurons (scale bar=50 μm). (H) Relative NeuN+ cell density in T1DM CIRI vehicle-treated group (n=5) and T1DM CIRI melatonin-treated group (n=4). * $P<0.05$, ** $P<0.005$ and *** $P<0.001$ between groups.

and Cheung, 2023).

Potential mechanisms of T1DM-mediated exacerbation of CIRI at 72 h may be revealed by comparing between NG CIRI group and T1DM CIRI group. Unlike our reported findings of T1DM-aggravated further increase in cytochrome C level at 24 h post-CIRI (Xu and Cheung, 2023), the present results revealed no significant difference in cerebral cortical levels of cytochrome C between NG CIRI group and T1DM group at 72 h post-CIRI. In line with our reported findings at 24 h post-CIRI (Xu and Cheung, 2023), the present results also revealed no significant difference in cerebral cortical levels of caspase-3-specific 120 kDa SBDP and calpain-specific 145 kDa SBDP between NG CIRI group and T1DM CIRI group at 72 h post-CIRI. Taking together, it is less likely that T1DM would exacerbate CIRI at 72 h via an enhanced release of cytochrome C, an augmented activation of caspase-3 and an intensified activation of calpains in the cerebral cortex.

It has been reported that mitochondrial dysfunction is more pronounced during an early stage of reperfusion, leading to an insignificant increase in cytochrome C level at a later time after reperfusion (Wyss et al., 2019). As a 15-member family of calcium-activated cysteine proteases localized to the cytosol and mitochondria (Smith and Schnellmann, 2012), some calpains are activated during the processes of necrosis and apoptosis (Smith and Schnellmann, 2012; Xu and Cheung, 2023). Calpains are present in the mitochondria (Smith and Schnellmann, 2012). Calcium overload leads to mitochondrial calpain-1 cleavage of the sodium/calcium exchanger, contributing to persistent mitochondrial calcium accumulations (Smith and Schnellmann, 2012). Activated calpain 1 induces further cytochrome C release and apoptosis (Smith and Schnellmann, 2012). Caspase-3 is a crucial mediator of apoptosis (Wang, 2000). Nevertheless, suppression of the above processes should be beneficial in ameliorating CIRI in both NG and T1DM rats. As the present results reveal that these processes remain activated at 72 h after CIRI, persistent suppression may be more effective, and the treatment time window may be longer than 24 h. Further studies using T1DM rats should be conducted to evaluate other pathways as potential underlying mechanisms of T1DM-mediating exacerbation of CIRI.

Melatonin not only protects against CIRI (Feng et al., 2017; Liu et al., 2019; Pei et al., 2003) but also mediates beneficial effects via neural stem cells in other neurological diseases such as Parkinson's disease, spinal cord injury and neural tube defects (Yu et al., 2017). Our recent study reported anti-inflammatory and anti-apoptotic effects of a single IP dose of melatonin at 10 mg/kg given at 30 min before 75-min ischemia in alleviating T1DM-aggravated CIRI at 24 h (Xu and Cheung, 2023). In the present study, additional IP doses at 10 mg/kg were given at 24 and 48 h of reperfusion with evaluation of CIRI at 72 h. When compared to T1DM CIRI vehicle-treated group, 3 doses of melatonin alleviated the T1DM-aggravated CIRI at 72 h so that there was no significant difference in the EA-infarct volume, latency to fall off in rotarod test, mNSS and weight loss between from NG CIRI group and T1DM CIRI melatonin-treated group. Thus, melatonin at repeated doses protects against T1DM-aggravated CIRI at 72 h.

Regarding the underlying beneficial mechanisms, melatonin treatment decreased the cerebral cortical ratio of p-IκBα/IκBα and the cerebral cortical levels of cytochrome C, caspase-3-specific 120 kDa SBDP and calpain-specific 145 kDa SBDP in T1DM CIRI melatonin-treated group when compared with T1DM CIRI vehicle-treated group. Mitochondria and nucleus have higher concentrations of melatonin than other organelles (Venegas et al., 2012). Administration of a single dose of melatonin inhibits cytochrome C release and related apoptotic cascades at 24 h post-CIRI (Xu and Cheung, 2023). Administration of multiple doses of melatonin alleviates mitochondrial dysfunction as reflected by the present findings of a decreased release of cytochrome C at 72 h post-CIRI. Melatonin is a potent free radical scavenger capable of reducing free radical generation and removing reactive oxygen species to alleviate oxidative stress (Reiter et al., 2016). The alleviated oxidative

stress may contribute to the reduced mitochondrial dysfunction. The decreased release of cytochrome C would result in reduced formation of apoptosome which, in turn, would trigger caspase-3-mediated apoptosis. This is supported by the present results of reduced caspase-3-mediated 120 kDa SBDP at 72 h post-CIRI in T1DM rats treated with repeated doses of melatonin. Calpains are present in several cell types of the central nervous system. Increased calpain activities are seen in various neurological diseases, including seizure, epilepsy, and stroke (Venegas et al., 2012). The present findings of reduced the calpain-mediated 145 kDa SBDP at 72 h post-CIRI in T1DM rats treated with repeated doses of melatonin indicate decreased calpain activation and support the notion that melatonin is a calpain inhibitor.

In the present study, repeated doses of melatonin decreased iNOS+ cells and TUNEL+ apoptotic cells and increased NeuN+ neuronal cells but did not affect CD-68+ cells in the cerebral cortex at 72 h post-CIRI in T1DM rats. Our results are in keeping with the proposed beneficial effect of melatonin treatment in reducing brain damage partly via shifting the microglia phenotype from pro-inflammatory (i.e. iNOS+, CD-86+, interleukin (IL)-6+ and/or tumor necrosis factor (TNF)-α+) to anti-inflammatory (i.e. CD206+, Arginase (Arg)-1+, YM1/2+, transforming growth factor (TGF)-β+ and/or IL-10+) polarity (Liu et al., 2019). Nevertheless, we did not find any significant suppression of cerebral cortical expression of CD-68+ macrophage/microglia despite decreased expression of iNOS+ stained cells at 72 h post-CIRI in T1DM rats. A plausible explanation of the conflicting results is that CD-68, being a pan-macrophage marker, may not be specific enough to differentiate between pro-inflammatory (M1) and anti-inflammatory (M2) macrophage/microglia (Klar et al., 2018). In contrast, iNOS is a specific marker of pro-inflammatory macrophage/microglia (Pan et al., 2015). Polarized macrophages are differentiated by differential expressions of molecules such as iNOS, metalloproteinase, and Arg-1 (Barros et al., 2013). In principal, double staining with CD-68 and iNOS is highly specific for M1 macrophage/microglia (Klar et al., 2018). In reality, merging of CD-68+ and iNOS+ cells are not commonly seen in brain sections, suggesting iNOS expression in non-macrophage/microglia such as reactive glial cells (Barros et al., 2013). In any case, repeated doses of melatonin can reduce the post-CIRI increased cerebral cortical expression of pro-inflammatory iNOS+ cells in T1DM rats.

According to the present results, increased apoptosis may not play a specific role in T1DM-exacerbated CIRI at 72 h. Post-ischemia-reperfusion apoptosis plays a crucial role in both NG CIRI group and T1DM CIRI group. As a potent antioxidant and free radical scavenger, melatonin mediates potent protection against mitochondrial dysfunction. Administration of melatonin preserves mitochondrial membrane potential and mitochondrial complex I activity and therefore reduces cytochrome C release into cytosol (Yang et al., 2015). The present results of reduced cerebral cortical levels of cytochrome C, caspase-3-specific 120 kDa SBDP, calpain-specific 145 kDa SBDP, and a decreased cerebral cortical density of TUNEL+ apoptotic cells at 72 h post-CIRI in T1DM rats treated with multiple doses of melatonin confirm its beneficial effects in inhibition of post-CIRI apoptosis and/or necrosis (Wang, 2000), leading to an increased cerebral cortical density of NeuN+ neuronal cells at 72 h post-CIRI.

5. Conclusion

The present results have extended our previous observations in T1DM rats at 24 h post-CIRI. Hyperglycemic environment of T1DM aggravates CIRI at 72 h with larger infarct volume, worse neurological deficits and greater weight loss via persistent activation of NF-κB pathway activation. Melatonin at 10 mg/kg given at 30 minutes before and repeated at 24 and 48 h post-CIRI is neuroprotective against CIRI in T1DM rats at 72 h. The beneficial mechanisms of melatonin treatment include stabilization of NF-κB pathway and reduced mitochondrial cytochrome C release as well as reduction in inflammation, apoptosis and neuronal cell death.

Author contributions

Q.X. and R.T.F.C. were involved in development of the hypotheses and experimental design. Q.X. conducted the majority of the experiments. Q.X. and R.T.F.C. performed the data analyses. Q.X. drafted the manuscript. R.T.F.C. critically revised the manuscript. Q.X. and R.T.F.C. approved the final version of the manuscript.

Declaration of Competing Interest

The author Q.X. and R.T.F.C. declare no competing interest.

Acknowledgments

This research was supported by matching and donation funds (UGC Matching Grant, HKU, Hong Kong; SHAC Fund, HKU, Hong Kong; Cerebrovascular Research Fund, HKU, Hong Kong; Dr. William Mong Research Fund, HKU, Hong Kong; CRCG Internal Research Fund, HKU, Hong Kong; and Lee Man-Chiu Professorship in Neuroscience, HKU, Hong Kong) awarded to Professor R.T.F. Cheung.

References

Ali, T., Rahman, S.U., Hao, Q., et al., 2020. Melatonin prevents neuroinflammation and relieves depression by attenuating autophagy impairment through FOXO3a regulation. J. Pineal Res. 69 (2), e12667.
Atkinson, M.A., Eisenbarth, G.S., Michels, A.W., 2014. Type 1 diabetes. Lancet 383 (9911), 69–82.
Audzeyenka, I., Rachubik, P., Typiak, M., et al., 2021. Hyperglycemia alters mitochondrial respiration efficiency and mitophagy in human podocytes. Exp. Cell Res. 407 (1), 112758.
Barone, F., Price, W., White, R., Willette, R., Feuerstein, G., 1992. Genetic hypertension and increased susceptibility to cerebral ischemia. Neurosci. Biobehav. Rev. 16 (2), 219–233.
Barros, M.H.M., Hauck, F., Dreyer, J.H., Kempkes, B., Niedobitek, G., 2013. Macrophage polarisation: an immunohistochemical approach for identifying M1 and M2 macrophages. PLOS One 8 (11), e80908.
Beckman, J.A., Creager, M.A., Libby, P., 2002. Diabetes and atherosclerosis: epidemiology, pathophysiology, and management. JAMA 287 (19), 2570–2581.
Broughton, B.R., Reutens, D.C., Sobey, C.G., 2009. Apoptotic mechanisms after cerebral ischemia. Stroke 40 (5), e331–e339.
Chistiakov, D.A., Killingsworth, M.C., Myasoedova, V.A., Orekhov, A.N., Bobryshev, Y. V., 2017. CD68/macrosialin: not just a histochemical marker. Lab. Investig. 97 (1), 4–13.
Christophe, M., Nicolas, S., 2006. Mitochondria: a target for neuroprotective interventions in cerebral ischemia-reperfusion. Curr. Pharm. Des. 12 (6), 739–757.
Chukwuma, Sr.C., Tuomilehto, J., 1993. Diabetes and the risk of stroke. J. Diabetes its Complicat. 7 (4), 250–262.
Cui, C., Ye, X., Chopp, M., et al., 2016. miR-145 regulates diabetes-bone marrow stromal cell-induced neurorestorative effects in diabetes stroke rats. Stem Cells Transl. Med. 5 (12), 1656–1667.
Diener, H.-C., Hankey, G.J., 2020. Primary and secondary prevention of ischemic stroke and cerebral hemorrhage: JACC focus seminar. J. Am. Coll. Cardiol. 75 (15), 1804–1818.
Ding, W.-X., Shen, H.-M., Ong, C.-N., 2002. Calpain activation after mitochondrial permeability transition in microcystin-induced cell death in rat hepatocytes. Biochem. Biophys. Res. Commun. 291 (2), 321–331.
El-Sahar, A.E., Safar, M.M., Zaki, H.F., Attia, A.S., Ain-Shoka, A.A., 2015. Neuroprotective effects of pioglitazone against transient cerebral ischemic reperfusion injury in diabetic rats: modulation of antioxidant, anti-inflammatory, and anti-apoptotic biomarkers. Pharmacol. Rep. 67 (5), 901–906.
Feigin, V.L., Stark, B.A., Johnson, C.O., et al., 2021. Global, regional, and national burden of stroke and its risk factors, 1990–2019: a systematic analysis for the Global Burden of Disease Study 2019. Lancet Neurol. 20 (10), 795–820.
Feng, D., Wang, B., Wang, L., et al., 2017. Pre-ischemia melatonin treatment alleviated acute neuronal injury after ischemic stroke by inhibiting endoplasmic reticulum stress-dependent autophagy via PERK and IRE 1 signalings. J. Pineal Res. 62 (3), e12395.
Forbes, J.M., Cooper, M.E., 2013. Mechanisms of diabetic complications. Physiol. Rev. 93 (1), 137–188.
Furman, B.L., 2015. Streptozotocin-induced diabetic models in mice and rats. Curr. Protoc. Pharmacol. 70 (1), 5.47. 1–5.47. 20.
Goldin, A., Beckman, J.A., Schmidt, A.M., Creager, M.A., 2006. Advanced glycation end products: sparking the development of diabetic vascular injury. Circulation 114 (6), 597–605.
Hägg, S., Thorn, L.M., Forsblom, C.M., et al., 2014. Different risk factor profiles for ischemic and hemorrhagic stroke in type 1 diabetes mellitus. Stroke 45 (9), 2558–2562.

Hägg-Holmberg, S., Thorn, L.M., Forsblom, C.M., et al., 2017. Prognosis and its predictors after incident stroke in patients with type 1 diabetes. Diabetes Care 40 (10), 1394–1400.
Hardeland, R., 2018. Melatonin and inflammation—story of a double-edged blade. J. Pineal Res. 65 (4), e12525.
Harwood, S.M., Yaqoob, M.M., Allen, D.A., 2005. Caspase and calpain function in cell death: bridging the gap between apoptosis and necrosis. Ann. Clin. Biochem. 42 (6), 415–431.
Jia, J., Liu, Y., Zhang, X., Liu, X., Qi, J., 2013. Regulation of iNOS expression by NF-κB in human lens epithelial cells treated with high levels of glucose. Invest. Ophthalmol. Vis. Sci. 54 (7), 5070–5077.
Jouihan, S.A., Zuloaga, K.L., Zhang, W., et al., 2013. Role of soluble epoxide hydrolase in exacerbation of stroke by streptozotocin-induced type 1 diabetes mellitus. J. Cereb. Blood Flow. Metab. 33 (10), 1650–1656.
Klar, A.S., Michalak-Mićka, K., Biedermann, T., Simmen-Meuli, C., Reichmann, E., Meuli, M., 2018. Characterization of M1 and M2 polarization of macrophages in vascularized human dermo-epidermal skin substitutes in vivo. Pediatr. Surg. Int. 34 (2), 129–135.
Lee, S., Hong, Y., LEE, S.-R., CHANG, K.-T., HONG, Y., 2014. Comparison of surgical methods of transient middle cerebral artery occlusion between rats and mice. J. Vet. Med. Sci. 14–0258.
Lin, L., Wang, X., Yu, Z., 2016. Ischemia-reperfusion injury in the brain: mechanisms and potential therapeutic strategies. Biochem. Pharmacol.: Open Access 5 (4).
Liu, Z.J., Ran, Y.Y., Qie, S.Y., et al., 2019. Melatonin protects against ischemic stroke by modulating microglia/macrophage polarization toward anti-inflammatory phenotype through STAT3 pathway. CNS Neurosci. Ther. 25 (12), 1353–1362.
Mendelson, S.J., Prabhakaran, S., 2021. Diagnosis and management of transient ischemic attack and acute ischemic stroke: a review. JAMA 325 (11), 1088–1098.
Noshahr, Z.S., Salmani, H., Khajavi Rad, A., Sahebkar, A., 2020. Animal models of diabetes-associated renal injury. J. Diabetes Res. 2020.
Nouraee, C., Fisher, M., Di Napoli, M., et al., 2019. A brief review of edema-adjusted infarct volume measurement techniques for rodent focal cerebral ischemia models with practical recommendations. J. Vasc. Interv. Neurol. 10 (3), 38.
Pan, J., Jin, J.-l, Ge, H.-m, et al., 2015. Malibatol A regulates microglia M1/M2 polarization in experimental stroke in a PPARγ-dependent manner. J. Neuroinflamm. 12 (1), 1–11.
Pei, Z., Pang, S.F., Cheung, R.T.F., 2003. Administration of melatonin after onset of ischemia reduces the volume of cerebral infarction in a rat middle cerebral artery occlusion stroke model. Stroke 34 (3), 770–775.
Rehman, S.U., Ikram, M., Ullah, N., et al., 2019. Neurological enhancement effects of melatonin against brain injury-induced oxidative stress, neuroinflammation, and neurodegeneration via AMPK/CREB signaling. Cells 8 (7), 760.
Reiter, R.J., Mayo, J.C., Tan, D.X., Sainz, R.M., Alatorre-Jimenez, M., Qin, L., 2016. Melatonin as an antioxidant: under promises but over delivers. J. Pineal Res. 61 (3), 253–278.
Samantaray, S., Sribnick, E.A., Das, A., et al., 2008. Melatonin attenuates calpain upregulation, axonal damage and neuronal death in spinal cord injury in rats. J. Pineal Res. 44 (4), 348–357.
Schaar, K.L., Brenneman, M.M., Savitz, S.I., 2010. Functional assessments in the rodent stroke model. Exp. Transl. Stroke Med. 2 (1), 13.
Smith, M.A., Schnellmann, R.G., 2012. Calpains, mitochondria, and apoptosis. Cardiovasc. Res. 96 (1), 32–37.
Söderpalm, B., Eriksson, E., Engel, J.A., 1989. Anticonflict and rotarod impairing effects of alprazolam and diazepam in rat after acute and subchronic administration. Prog. Neuro Psychopharmacol. Biol. Psychiatry 13 (1-2), 269–283.
Sundquist, K., Li, X., 2006. Type 1 diabetes as a risk factor for stroke in men and women aged 15–49: a nationwide study from Sweden. Diabet. Med. 23 (11), 1261–1267.
Tamtaji, O.R., Mirhosseini, N., Reiter, R.J., Azami, A., Asemi, Z., 2019. Melatonin, a calpain inhibitor in the central nervous system: current status and future perspectives. J. Cell. Physiol. 234 (2), 1001–1007.
Toung, T.K., Hurn, P.D., Traystman, R.J., Sieber, F.E., 2000. Estrogen decreases infarct size after temporary focal ischemia in a genetic model of type 1 diabetes mellitus. Stroke 31 (11), 2701–2706.
Venegas, C., García, J.A., Escames, G., et al., 2012. Extrapineal melatonin: analysis of its subcellular distribution and daily fluctuations. J. Pineal Res. 52 (2), 217–227.
Viatour, P., Merville, M.-P., Bours, V., Chariot, A., 2005. Phosphorylation of NF-κB and IκB proteins: implications in cancer and inflammation. Trends Biochem. Sci. 30 (1), 43–52.
Wang, K.K., 2000. Calpain and caspase: can you tell the difference. Trends Neurosci. 23 (1), 20–26.
Wautier, M.-P., Chappey, O., Corda, S., Stern, D.M., Schmidt, A.M., Wautier, J.-L., 2001. Activation of NADPH oxidase by AGE links oxidant stress to altered gene expression via RAGE. Am. J. Physiol., Endocrinol. Metab. 280 (5), E685–E694.
Wyss, R.K., Méndez-Carmona, N., Sanz, M.-N., et al., 2019. Mitochondrial integrity during early reperfusion in an isolated rat heart model of donation after circulatory death—consequences of ischemic duration. J. Heart Lung Transplant. 38 (6), 647–657.
Xu, Q., Cheung, R.T.F., 2023. Melatonin mitigates type 1 diabetes-aggravated cerebral ischemia-reperfusion injury through anti-inflammatory and anti-apoptotic effects. Brain Behav. 13 (9), e3118.
Yan, T., Chopp, M., Ye, X., et al., 2012. Niaspan increases axonal remodeling after stroke in type 1 diabetes rats. Neurobiol. Dis. 46 (1), 157–164.
Yan, T., Venkat, P., Chopp, M., et al., 2018. APX3330 promotes neurorestorative effects after stroke in type one diabetic rats. Aging Dis. 9 (3), 453.
Yang, Y., Jiang, S., Dong, Y., et al., 2015. Melatonin prevents cell death and mitochondrial dysfunction via a SIRT 1-dependent mechanism during ischemic-stroke in mice. J. Pineal Res. 58 (1), 61–70.
Yawoot, N., Govitrapong, P., Tocharus, C., Tocharus, J., 2021. Ischemic stroke, obesity, and the anti-inflammatory role of melatonin. Biofactors 47 (1), 41–58.
Yu, X., Li, Z., Zheng, H., Ho, J., Chan, M.T., Wu, W.K.K., 2017. Protective roles of melatonin in central nervous system diseases by regulation of neural stem cells. Cell Prolif. 50 (2), e12323.
Zhang, Y., Bhavnani, B.R., 2006. Glutamate-induced apoptosis in neuronal cells is mediated via caspase-dependent and independent mechanisms involving calpain and caspase-3 proteases as well as apoptosis inducing factor (AIF) and this process is inhibited by equine estrogens. BMC Neurosci. 7 (1), 49.